



## The Formability and Elongation of Aluminum Alloys AA5083 and AA3003 for Micro-Truss Sandwiches Manufacturing

Arwa F. Tawfeeq<sup>a\*</sup>, Matthew R. Barnett<sup>b</sup>

<sup>a</sup> Department of Materials Engineering, University of Technology, Baghdad, Iraq, Email address: 130207@uotechnology.edu.iq, arwatawfeeq@yahoo.com

<sup>b</sup> Institute for Frontier Materials, Deakin University, Geelong, Australia, Email address: matthew.barnett@deakin.edu.au

\*Corresponding author.

Submitted: 02/09/2019

Accepted: 27/04/2020

Published: 25/09/2020

### KEY WORDS

Aluminum alloy 5083,  
aluminum alloy 3003,  
micro-truss, tensile,  
formability

### ABSTRACT

*The development in the manufacturing of micro-truss structures has demonstrated the effectiveness of brazing for assembling these sandwiches, which opens new opportunities for cost-effective and high-quality truss manufacturing. An evolving idea in micro-truss manufacturing is the possibility of forming these structures in different shapes with the aid of elevated temperature. This work investigates the formability and elongation of aluminum alloy sheets typically used for micro-truss manufacturing, namely AA5083 and AA3003. Tensile tests were performed at a temperature in the range of 25-500 °C and strain rate in the range of  $2 \times 10^{-4}$  -  $10^{-2}$  s<sup>-1</sup>. The results showed that the clad layer in AA3003 exhibited an insignificant effect on the formability and elongation of AA3003. The formability of the two alloys was improved significantly with values of  $m$  as high as 0.4 and 0.13 for AA5083 and AA3003 at 500 °C. While the elongation of both AA5083 and AA3003 was improved at a higher temperature, the elongation of AA5083 was inversely related to strain rate. It was concluded that the higher the temperature is the better the formability and elongation of the two alloys but at the expense of work hardening. This suggests a trade-off situation between formability and strength.*

**How to cite this article:** A. F. Tawfeeq, M. R., Barnett, "The Formability and Elongation of Aluminum Alloys AA5083 and AA3003 for Micro-Truss Sandwiches Manufacturing," Engineering and Technology Journal, Vol 38. , Part A, No. 09, pp. 1396-1405, 2020.  
DOI: <https://doi.org/10.30684/etj.v38i9A.556>

This is an open access article under the CC BY 4.0 license <http://creativecommons.org/licenses/by/4.0>

## 1. INTRODUCTION

Transport applications frequently need metal structures that are stiff, strong, tough and light. The choices that best achieve this are often the light alloys [1]. Cellular metal structures, that are either stochastic (metal foams) [2, 3] or periodic (PCMs) [1, 4, 5] are highly attractive types of lightweight metals that are becoming increasingly utilized in the industry [6]. Periodic cellular structures

typically display better property profiles than stochastic cellular materials, at equivalent densities. The last two decades have witnessed the proposal of PCMs for a wide range of engineering applications such as in electric sensing and actuation [7, 8], aerospace [9], underwater shock loading [10-12], heat transfer [13-16], energy absorption [6, 17], and aircraft wings manufacturing [18]. Micro-truss panel structures are one example. These structures are created using an interconnected network of solid struts acting as columns and ties [19-21]. Cost-effective methods for micro-truss production have also been developed, such as casting-based procedures [22], however, the product suffers of structural defects that, for some applications, cause poor performance and early failure. Another method for manufacturing micro-trusses is by brazing. This method has attracted increasing attention due to its flexibility, lower cost, and high-strength joints produced after brazing. In this method, the perforated metal sheets (usually aluminum) are assembled by brazing using a filler (brazing alloy). During brazing, the structures are subjected to elevated temperatures to produce high-quality brazed joints. This process will cause annealing which will result in a loss of some work hardening of the material. However, when the metals are subjected to elevated temperature its formability and elongation improved. This provides the possibility of manufacturing micro-trusses in shapes and forms that are difficult to produce at ambient temperature without introducing undesirable defects. Therefore, it is important to characterize the formability and elongation of these sheets and joints brazed at conditions relevant to micro-truss manufacturing. This work presents the ductility and elongation results of two aluminum alloys, namely AA5083 and AA3003, commonly used in manufacturing micro-trusses. Important parameters related to the formability and elongation of these alloys (i.e. strain hardening exponent, strength hardening coefficient, and strain rate sensitivity index) were determined.

## 2. EXPERIMENTAL

### I. Materials

Two aluminum alloys were used in this work. The first alloy is AA3003, which is representative of the aluminum alloys that would be used to manufacture commercial micro-truss structures. The AA3003 was supplied in sheets of 1.5 mm thickness with a cladding of AA3434 (Figure 1). Two types of this alloy were examined, single-face clad (to be designated as an AA3003-1 side clad throughout this work) and both-faces clad (to be designated as AA3003-2 side clad). The chemical composition analysis was performed using a Spectro MAXx Analyzer. The chemical composition analysis given in Table 1 shows the concentrations (in weight %) of six major elements. The metallographic examination was performed on AA3003 to determine the thickness of the clad layer and found to be in the range of 127-132  $\mu\text{m}$ . The second alloy is AA5083, which was supplied as 20 mm thick plates.

TABLE I: Chemical compositions of the alloys used in the present study

Alloy	Base Alloy - AA5083					
Element	Al	Mg	Mn	Fe	Si	Cr
Concentration (wt%)	94.3	4.26	0.845	0.299	0.119	0.069
Alloy	Base Alloy - AA3003					
AA3003-1 Side Clad/face A						
Element	Al	Si	Fe	Sb	Cu	Ga
Concentration (wt%)	91.2	8.50	0.187	0.046	0.014	0.013
AA3003-1 Side Clad/face B						
Element	Al	Mn	Cu	Si	Fe	Ti
Concentration (wt%)	98.2	0.838	0.283	0.205	0.203	0.160
AA3003-2 Side Clad/face A						
Element	Al	Si	Fe	Sb	Hg	Mg
Concentration (wt%)	91.6	8.10	0.193	0.051	0.012	0.006
AA3003-2 Side Clad/face B						
Element	Al	Si	Fe	Sb	Hg	Ga
Concentration (wt%)	91.4	8.31	0.190	0.05	0.012	0.005

## II. Dog-bone sample manufacturing

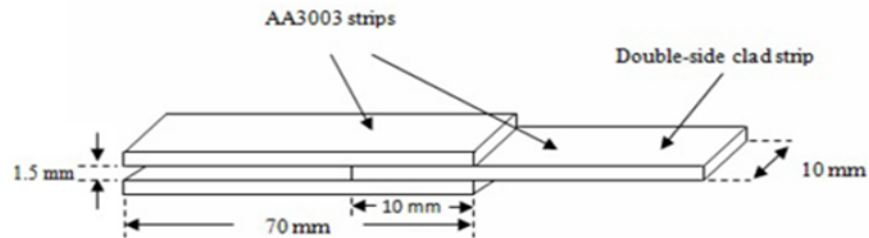


Figure 1: Double-lap joint

For a successful brazing process, it is essential to determine the best brazing conditions. Lap-joint specimens were manufactured from AA3003-1 and 2 sides clad. This type of joint provides the possibility of optimizing important parameters without compromising real micro-truss structures. In addition, lap joints are easy to handle and test and can provide reliable data that would be helpful for brazing micro-truss structures. Figure 1 shows a schematic of a lap joint with the dimensions used in this work. The determination of the best brazing condition was decided based on brazed joint strength. Brazing temperatures were 595 °C, 600 °C, and 605 °C. Three specimens were brazed at each temperature to determine the reproducibility. The furnace was brought to the desired brazing condition prior to placing the sample in the furnace to ensure a reliable brazing condition.

The preparation of specimens for brazing included the following steps: The strips were ground and polished using a grinding machine (Struers Rotopol-1) in order to obtain parallel and smooth surfaces, then cleaned using a hot detergent solution to remove all grease, oil and dirt from the surfaces of the metal, followed by washing with ethanol for 2 min and left to dry in air. The strips were then coated with flux and submitted to braze in an argon gas atmosphere. After reaching the desired brazing temperature, the specimens were removed, air-cooled, and cleaned using a metal brush to remove any residue. The maximum brazing temperature was selected so as to be close to the liquidus temperature of AA4343, reported as 612 °C [19], while significantly below the solidus temperature of AA3003 that is about 643 °C [23]. Brazed double-lap joints were shaped to a dog-bone configuration using a CNC machine (TRIAC-Fanuc ATC-GE Fanuc Series O-M) and according to ASTM D3528, as shown in Figure 2, to examine the mechanical strength of the brazed joint. Uniaxial tensile tests were performed on a 30kN Instron machine. Tensile tests were performed at room temperature with a crosshead speed of 0.1 mm/s (equivalent to a strain rate of  $3 \times 10^{-3} \text{ s}^{-1}$ ). The test was allowed to continue until the specimen failed. The failed specimens exhibited a similar failure where the fracture occurred outside the brazed joint regardless of brazing condition or cladding. An example is given in Figure 3. This behavior indicates that the plastic strain is distributed entirely outside the brazed joint and no significant plastic yield was formed within the brazed joint.

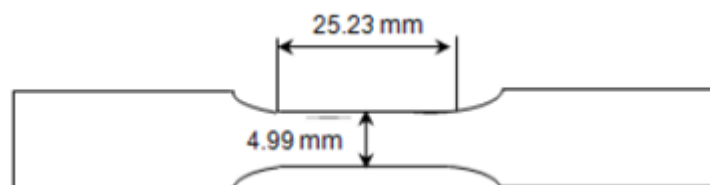


Figure 2: Dog-bone configuration of the tensile double-lap joint specimen.

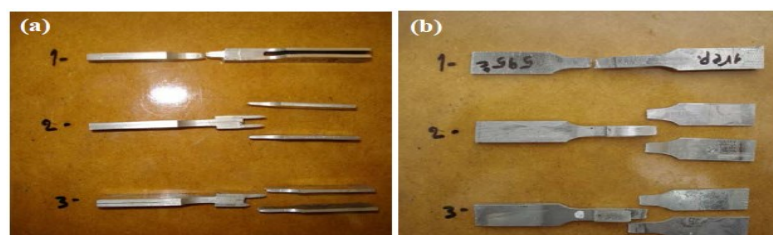


Figure 3: Failed double-lap joints of the AA3003-2 side clad brazed at 595 °C; (a) side and (b) top view.

### III. Experimental Set-Up

The test machine used to execute all experiments was the 30kN Instron. The machine is connected to a data acquisition system to enable controlling the test conditions by computer, e.g., strain rate or overhead speed, strain, temperature, specimen dimensions, etc. The heating system used in the elevated temperature experiments was a heating rig connected to a power control panel. The choice of the heating rig in these experiments is based on the size of the interior space of the machine where the rig was to be installed.

### IV. Methods

Tensile tests were carried out according to ASTM E8 specifications using the 30kN Instron (Figure 4). At room temperature, the test was performed with an extensometer (non-contact model 2663-821). The progress of the test was monitored using a video camera to visually analyze the behavior of the specimen during the test. This also enabled obtaining more precise strain level measurements. The strain level was measured by contrasting the upper and lower limits of the gauge length along with the specimen with white dots using a marking pen. At room temperature the test was conducted on AA5083, parent AA3003-1 and 2 sides clad, and the annealed AA3003-1 and 2 sides clad. The test was conducted at strain rates of  $2 \times 10^{-4}$ ,  $10^{-3}$ ,  $10^{-2}$  and  $10^{-1} \text{ s}^{-1}$ , whereas the annealed specimen was tested at  $10^{-3} \text{ s}^{-1}$  and  $10^{-2} \text{ s}^{-1}$ . For tests at elevated temperatures, the test temperature was varied from 100 to 500 °C. Three tensile strain rates were applied, namely;  $2 \times 10^{-4}$ ,  $10^{-3}$  and  $10^{-2} \text{ s}^{-1}$ . Strain rate jump tests were also carried out. The flow stress was reported instantaneously before and after the jump in rates. The base strain rate was constant at  $2 \times 10^{-4} \text{ s}^{-1}$ . The strain rate was changed at plastic strains of  $\sim 3\%$  and  $15\%$ , to a strain rate of  $10^{-3} \text{ s}^{-1}$ , and at  $9\%$  and  $21\%$  for a strain rate of  $10^{-2} \text{ s}^{-1}$ . Prior to the test, the specimens were subjected to  $\sim 2$  min preheating to obtain a stable target temperature. Three tests were performed at each temperature to reduce the scatter of data.

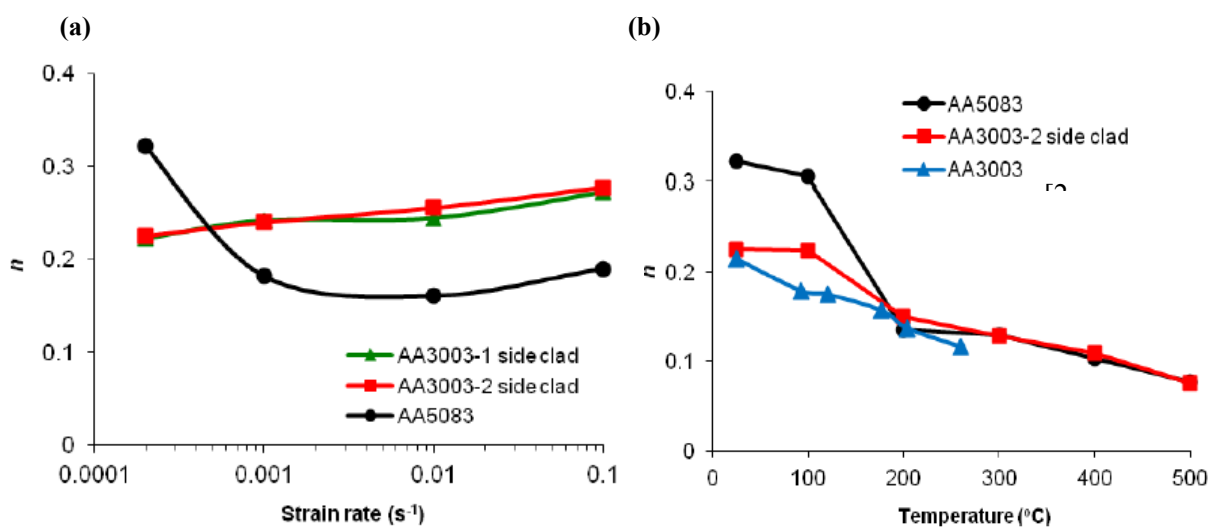


Figure 4: The dependency of strain hardening exponent on; (a) strain rate at 25 °C, and (b) temperature at strain rate  $2 \times 10^{-4} \text{ s}^{-1}$ .

### V. Analysis

The values of strain hardening exponent ( $n$ ) and strength hardening coefficient ( $K$ ) are determined for the two alloys by fitting a power law given in equation (1) to the uniform strain region of the true stress-strain curves [24]:

$$\sigma = (K\varepsilon^n) \quad (1)$$

Where  $\sigma$  is the stress (Mpa) and  $\epsilon$  is the strain. The strain rate sensitivity index ( $m$ ) is calculated using equation (3) derived from equation (2) [25].

$$\sigma = C \cdot \dot{\epsilon}^m \quad (2)$$

$$m = \frac{\Delta \ln(\sigma)}{\Delta \ln(\dot{\epsilon})} \quad (3)$$

Where  $\dot{\epsilon}$  is strain rate.

### 3. RESULTS

#### I. Strain hardening exponent ( $n$ ) and strength hardening coefficient ( $K$ )

Strain hardening exponent ( $n$ ) and strength hardening coefficient are determined by Eq. (1). Figure 4a exhibits the dependency of  $n$  as a function of strain rate at room temperature for both alloys, whereas Figure 4b shows the dependency of  $n$  on the temperature at a strain rate of  $2 \times 10^{-4} \text{ s}^{-1}$ . It can be seen in the figure that  $n$  values of AA3003 vary in a linear fashion from 0.26 to 0.28 when the strain rate is increased from  $2 \times 10^{-4} \text{ s}^{-1}$  to  $10^{-2} \text{ s}^{-1}$ . In the case of AA5083, the trend is different,  $n$  changed nonlinearly from 0.32 to 0.19 when the strain rate increased from  $2 \times 10^{-4}$  to  $10^{-1} \text{ s}^{-1}$ . It is apparent that AA5083 shows higher  $n$  values than AA3003 at ambient temperatures. For temperatures greater than  $200 \text{ }^\circ\text{C}$  the two alloys display similar values for  $n$ , as shown in Figure 4b. The trend of  $n$  values of AA3003 is found to be consistent with that obtained by Abedrabbo et al. [26] who reported a value of 0.22 at  $25 \text{ }^\circ\text{C}$  and a strain rate of  $0.008 \text{ s}^{-1}$ , while a later study by Ahmadi et al. [27] reported an AA3003-2 side clad value of 0.17 for a hardened AA3003 at a cross-head speed of  $0.017 \text{ mm/s}$  (the current strain rates of  $2 \times 10^{-4}$  and  $10^{-1} \text{ s}^{-1}$  correspond to the cross-head speed of  $0.005$  and  $2.5 \text{ mm/s}$ , respectively). The value of  $K$  in Eq. (1) is plotted in Figure 5. A steep decline in  $K$  with increasing temperature is seen with convergence between the two alloys evident at  $400 \text{ }^\circ\text{C}$ .

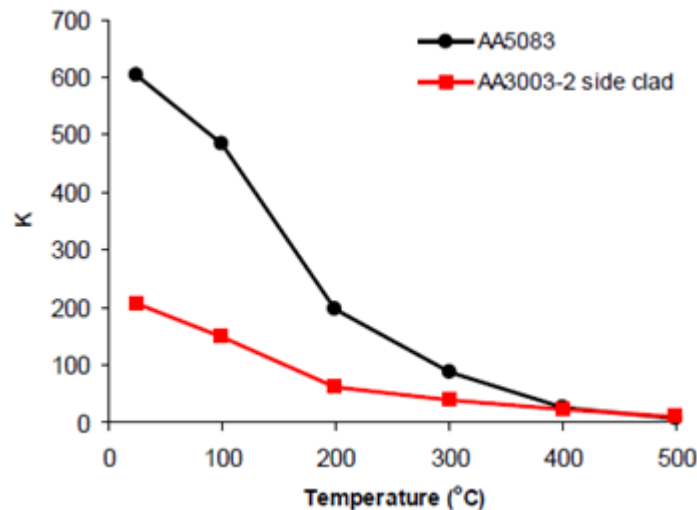


Figure 5: The dependency of strength hardening coefficient on the temperature at a strain rate of  $2 \times 10^{-4} \text{ s}^{-1}$ .

#### II. Strain Rate Sensitivity Index ( $m$ )

The strain rate sensitivity index ( $m$ ) is plotted in Figure 6. The values of  $m$  were obtained using the jump-test method and comparison of curves obtained at different strain rates. Assuming a power-law stress-strain-strain rate Eq. (3) where  $C$  is a constant.  $m$  was determined from the slope of the log-log plots using Eq. (2) at various strain rates between  $2 \times 10^{-4}$  and  $10^{-1} \text{ s}^{-1}$  for a fixed strain level of 5% (after Benallie et al. [28] and Grytten et al. [29]). The values are shown in Figure 6 display a reasonable agreement between the two techniques. The values are also compare reasonably well with

the literature, as shown in the Figure. However, it can be seen in Figure 7 that  $m$  values of AA5083 are higher than those of AA3003 at temperatures higher than 300 °C.

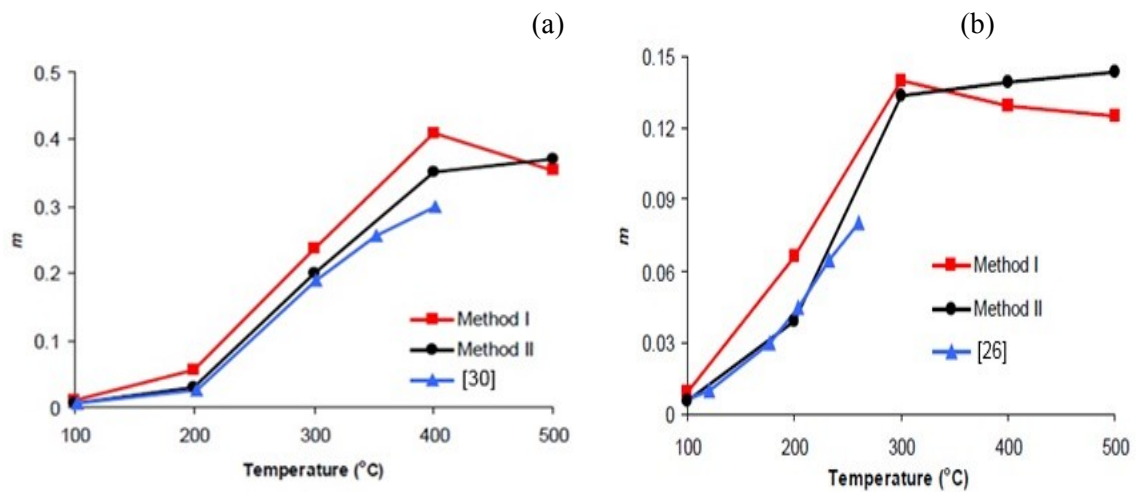


Figure 6: Strain rate sensitivity calculated according to rate jump ( $2 \times 10^{-4}$  to  $10^{-2}$  s $^{-1}$ ) – method I; and from  $\dot{\epsilon}$ - $\sigma$  data for different  $\dot{\epsilon}$  ( $2 \times 10^{-4}$  to  $10^{-2}$  s $^{-1}$ ) – method II; (a) AA5083, and (b) AA3003.

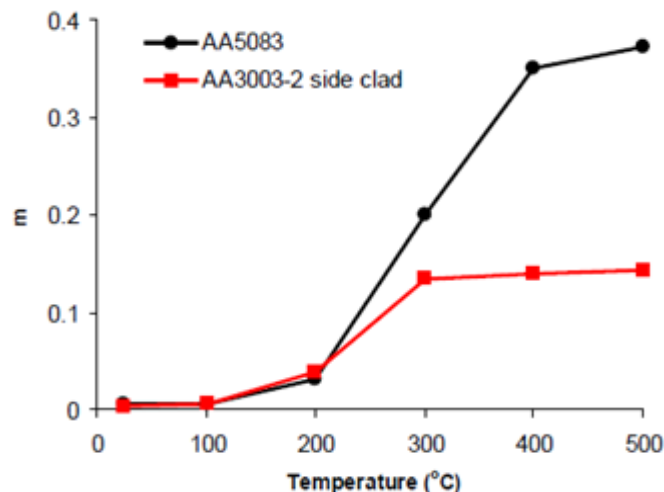


Figure 7: A comparison of  $m$  for AA5083 and AA3003-2 side clad.

The response of elongation to strain rate for AA5083 and AA3003 at 25 °C is shown in Figures 8 and 9, respectively. Total elongation to failure (TE) and uniform elongation (UE) of AA5083 decreased from 18.5% and 16.2% at  $2 \times 10^{-4}$  s $^{-1}$  to 7.4% and 6.7% at  $10^{-1}$  s $^{-1}$ , respectively. By contrast, the TE and UE of AA3003 are relatively insensitive to the strain rate at room temperature. The AA3003 values are also higher than those for AA5083. The elongation of these alloys is highly dependent on temperature. Figures 10 and 11 illustrate the elongation response of AA5083 and AA3003, respectively, at a strain rate  $2 \times 10^{-4}$  s $^{-1}$  and temperature in the range of 25-500 °C. It is noticeable that UE decreases at temperatures higher than 100 °C, and diminishes at temperatures higher than 300 °C. It must be highlighted that UE is the useful elongation for micro-truss forming as it ensures a uniform forming of assembled parts in the truss while the structure is deformed to the desired shape.

### III. Elongation

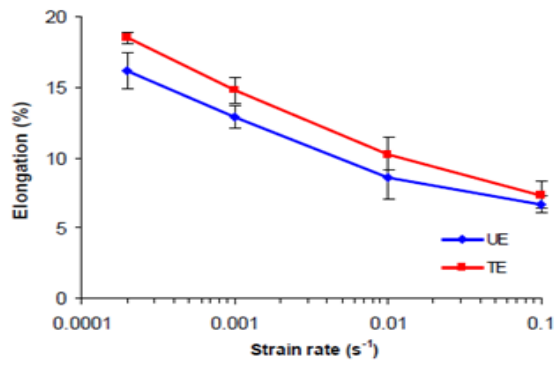


Figure 8: Effect of strain rate on the elongation of AA5083 at 25 °C.

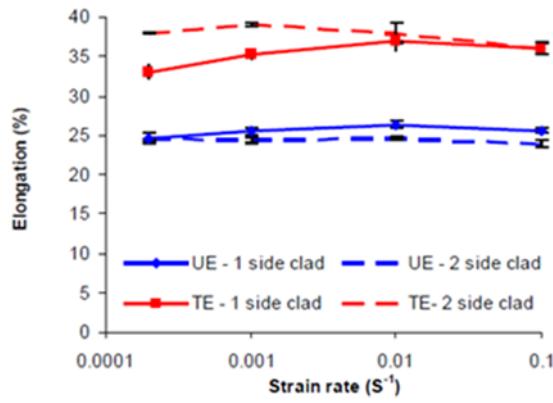


Figure 9: Effect of strain rate on the elongation of AA3003 at 25 °C.

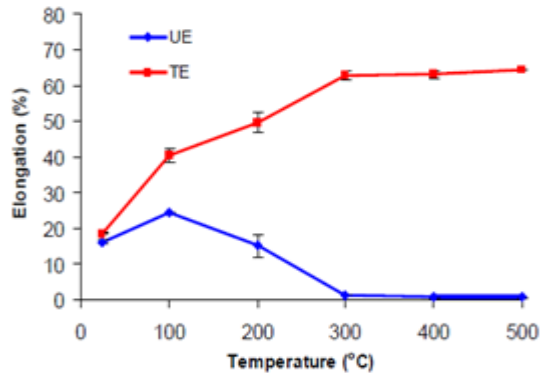


Figure 10: Elongation of AA5083 as a function of temperature at the strain rate of 2x10<sup>-4</sup> s<sup>-1</sup>.

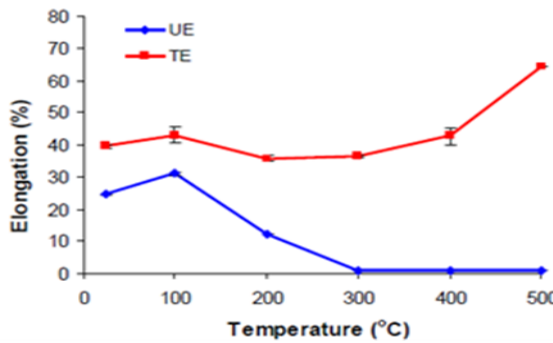


Figure 11: Elongation of AA3003-2 side clad as a function of temperature at strain

#### 4. DISCUSSION

The current findings show that the clad layer has an insignificant effect on the elongation of AA3003. This implies that the current alloys (AA3003 -1 and 2 sides clad) can be used without compromise in the elongation due to the clad layer. Unlike AA3003 where  $n$  values were insensitive to strain rate, AA5083 exhibited  $n$  values that are sensitive to strain rate. Accordingly, the deformed nature of AA5083 can be between plastic and elastic tuned by the strain rate, and as a result the value of  $n$ . Strain rate sensitivity ( $m$ ) for all specimens in this work was also obtained over extended ranges of temperature and strain rate, compared to previous works [26,30]. For instance, at 25 °C the tests were performed at a strain rate range of  $10^{-4}$  to  $10^{-1}$  s $^{-1}$ , whereas at temperatures >100 °C the tests were performed at a strain rate range of  $10^{-4}$  to  $10^{-2}$  s $^{-1}$ . These conditions are wider than those applied in Lloyd's work [30] who performed tests at a temperature range of 20-400 °C and strain rate of  $1.6 \times 10^{-4}$  s $^{-1}$ . Furthermore, in the work of Abedrabbo et al. [26], tensile tests were performed at a temperature range of 25-260 °C and the strain rate of  $8 \times 10^{-3}$  s $^{-1}$ . Clearly, the current conditions are more comprehensive than those applied in previous work. The difference in  $m$  values of AA5083 and AA3003 at temperatures higher than 300 °C, shown in Figure 7, is attributed to the difference in alloying elements, e.g. Mg and Fe [30,31], in the two alloys as shown in Table 1. In general, higher  $m$  promotes more uniform buckling of struts, which decreases stress flow localization, which is a desirable feature in the forming processes of trusses. The elongation of AA5083 (Figure 8) was limited compared to that of AA3003 (Figure 9). The limitation can be rationalized by the effect of alloy's chemical composition. Luo et al. [31] showed that increasing Fe from 0.03% to 0.23% in AA5083 reduced the ductility significantly. Accordingly, it appears reasonable that the current alloy with a Fe content of 0.3% exhibits a reduced ductility. Other studies [32, 33, and 34] showed that high elongations can be obtained with AA5083 by reducing Fe and Si content in the alloy. It is also apparent in Figure 9 that both AA3003-1 and 2 sides clad did not differ significantly in their elongation response to the strain rate change, which is in favor of the previous conclusion on the insignificant effect of the clad layer on alloy's properties. The UE of AA5083 and AA3003, shown in Figures 10 and 11, drops with temperature, reflecting a drop-in work hardening due to increased recovery. By 300 °C, the UE is negligible. The absence of work hardening at higher temperatures is likely to be significant for pyramidal truss structures, in which plastic buckling is important.

#### 5. CONCLUSIONS

The formability and elongation properties of AA5083 and AA3003-1 and 2 sides clad were determined as a function of temperature in the range of 25-500 °C and strain rate in the range of  $2 \times 10^{-4}$  -  $10^{-2}$  s $^{-1}$ . The main conclusions are:

1. Clad layer of AA3003 did not have any significant effect on the  $n$ ,  $K$ ,  $m$  and elongation. Accordingly, either AA3003-1 or AA3003-2 side clad can be used.
2. Uniform elongation also dropped away at 300 °C for both AA5083 and AA3003, reflecting a loss of work hardening capacity.
3. For AA5083, the elongation was sensitive to the strain rate. The higher the strain rate is the lower the achievable elongation. While AA3003 exhibited an elongation that is insensitive to strain rate.
4. At temperatures higher than 100 °C, the higher the temperature is the higher the strain-hardening exponent ( $n$ ) for both alloys.
5. Strain rate sensitivity index ( $m$ ) is more sensitive to a temperature higher than 200 °C, the higher the temperature is the higher the  $m$  value. This suggests enhanced formability. AA5083 exhibited higher formability than AA3003.

Despite the fact that increasing the temperature has a useful effect on the formability and elongation of AA5083 and AA3003, the work hardening of the alloys is highly compromised at elevated temperatures. Thus, a trade-off situation is to be considered during the manufacturing of such structures.

#### 6. REFERENCES

- [1] H.N.G. Wadley, "Cellular metals manufacturing," Advanced Engineering Materials, 4(10), PP.726-73, 2002.

- [2] M.F. Ashby, A.G. Evans, N.A. Fleck, L.J. Gibson, J.W. Hutchinson, and H.N.G. Wadley, "Metal Foams: A Design Guide," Butterworth-Heinemann, (Massachusetts, United States), 2000.
- [3] D.T. Queheillalt, Y. Katsumura, and H.N.G. Wadley, "Synthesis of stochastic open cell N-Based foams," *Scripta Materialia*, 50, PP.313-317, 2004.
- [4] A.G. Evans, J.W. Hutchinson, N.A. Fleck, M.F. Ashby, and H.N.G. Wadley, "The topological design of multifunctional cellular metals," *Progress in Materials Science*, 46, PP. 309-327, 2001.
- [5] H.N.G. Wadley, N.A. Fleck, and A.G. Evans, "Fabrication and structural performance of periodic cellular metal sandwich structures," *Composites Science and Technology*, 63, PP. 2331-2343, 2003.
- [6] C.J. Yungwirth, D.D. Radford, M. Aronson, and H.N.G. Wadley, "Experiment assessment of the ballistic response of composite pyramidal lattice truss structures," *Composites: Part B*, 39, PP. 556-569, 2008.
- [7] E.H. Anderson and N.W. Hagood, "Simultaneous piezoelectric sensing actuation: analysis and application to controlled structures," *Journal of Sound and Vibration*, 174 (5), pp. 617-639, 1994.
- [8] R.G. Hutchinson, N. Wicks, A.G. Evans, N.A. Fleck, and J.W. Hutchinson, "Kagome plate structures for actuation," *International Journal of Solids and Structures*, 40, PP. 6969-6980, 2003.
- [9] E.F. Crawley, "Intelligent structures for aerospace: a technology overview and assessment", *AIAA Journal*, 32 (8): pp. 1689-1699, 1994.
- [10] V.S. Deshpande and N.A. Fleck, "One-dimensional response of sandwich plates to underwater shock loading," *Journal of the Mechanics and Physics of Solids*, 53, pp. 2347-2383, 2005.
- [11] Y. Liang, A. V. Spuskanyuk, S. E. Flores, D. R. Hayhurst J. W. Hutchinson, R. M. McMeeking, and A. G. Evans, "The response of metallic sandwich panels to water blast," *Journal of Applied Mechanics*, 74, pp. 81-99, 2007.
- [12] K.P. Dharmasena, D.T. Queheillalt, H. N.G. Wadley, P. Dudt, Y. Chen, D. Knight, Z. Wei, and A.G. Evans, "Dynamic response of a multilayer prismatic structure to impulsive loads incident from water," *International Journal of Impact Engineering*, 36, pp. 632-643, 2009.
- [13] S. Gu, T.J. Lu, and A.G. Evans, "On the design of two-dimensional cellular metals for combined heat dissipation and structural load capacity," *International Journal of Heat and Mass Transfer*, 44, pp. 2163-2175, 2001.
- [14] J. Tian, T. Kim, T.J. Lu, H.P. Hodson, D.T. Queheillalt, and H.N.G. Wadley, "The effects of topology upon fluid-flow and heat-transfer within cellular cooper structures," *International Journal of Heat and Mass Transfer*, 47, pp. 3171-3186, 2004.
- [15] T. Wen, J. Tian, T.J. Lu, D.T. Queheillalt, and H.N.G. Wadley, "Forced convection in metallic honeycomb structures," *International Journal of Heat and Mass Transfer*, 49, pp. 3313-3324, 2006.
- [16] J. Tian, T.J. Lu, H.P. Hodson, D.T. Queheillalt, and H.N.G. Wadley, "Cross flow heat exchange to textile cellular metal core sandwich panels," *International Journal of Heat and Mass Transfer*, 50, pp. 2521-2536, 2007.
- [17] J.W. Hutchinson and Z. Xue, "Metal sandwich plates optimized for pressure impulses," *International Journal of Mechanical Sciences*, 47, pp. 545-569, 2005.
- [18] A.Y.N. Sofla, S.A. Meguid, K.T. Tan, and W.K. Yeo, "Shape morphing of aircraft wing: status and challenges," *Materials and Design*, 31, pp. 1284-1292, 2010.
- [19] L.J. Gibson and M.F. Ashby, "Cellular Solids Structure and Properties," 2nd ed., Cambridge University Press, United Kingdom, 1997.
- [20] T.J. Lu, H.A. Stone, and M.F. Ashby, "Heat transfer in open cell metal foams," *Acta Materialia*, 46 (10), pp. 3619-3635, 1998.
- [21] C. Chen, T.J. Lu and N.A. Fleck, "Effect of imperfections on the yielding of two-dimensional foams," *Journal of the Mechanics and Physics of Solids*, 47 (11), pp. 2235-2272, 1999.
- [22] N. Wicks and J.W. Hutchinson, "Optimal truss plates," *International Journal of Solids and Structures*, 38, pp. 5165-5183, 2001.
- [23] F. Côté, V.S. Deshpande, N.A. Fleck, and A.G. Evans, "The compressive and shear responses of corrugated and diamond lattice materials," *International Journal of Solids and Structures*, 43, pp. 6220-6242, 2006.

- [24] G.E. Dieter, "Mechanical Metallurgy," 3rd ed., McGraw-Hill, Boston, 1986.
- [25] I. Sabirov I., M. R. Barnett, Y. Estrin, and P. D. Hodgson, "The effect of strain rate on the deformation mechanisms and the strain rate sensitivity of an ultrafine-grained Al alloy," *Scripta Materialia*, 61, pp. 181-184, 2009.
- [26] N. Abedrabbo, F. Pourboghrat, and J. Carsley, "Forming of aluminum alloys at elevated temperatures – Part I: Material characterization," *International Journal of Plasticity*, 22, pp. 314–341, 2006.
- [27] S. Ahmadi, A.R. Eivani, and A. Akbarzadeh, "An experimental and theoretical study on the prediction of forming limit diagrams using new BBC yield criteria and M–K analysis," *Computational Materials Science*, 44 (4), pp. 1272–1280, 2009.
- [28] A. Benallal, T. Berstad, T. Børvik, O.S. Hopperstad, I. Koutiri, and R. Nogueira de Codes, "An experimental and numerical investigation of the behaviour of AA5083 aluminium alloy in presence of the Portevin–Le Chatelier effect," *International Journal of Plasticity*, 24, pp. 1916–1945, 2008.
- [29] F. Grytten, T. Børvik, O.S. Hopperstad, and M. Langseth, "Low velocity perforation of AA5083-H116 aluminium plates," *International Journal of Impact Engineering*, 36, pp. 597–610, 2009.
- [30] D.J. Lloyd, "The deformation of commercial aluminum-magnesium alloys," *Metallurgical Transactions A*, 11(8), pp. 1287-1294, 1980.
- [31] Y. Luo, C. Miller, G. Luckey, P. Friedman, and Y. Peng, "On practical forming limits in superplastic forming of aluminum sheet," *ASM International*, 16, pp. 274–283, 2007.
- [32] K. Kannan, C. H. Johnson, and C. H. Hamilton, "A study of superplasticity in a modified 5083 Al-Mg-Mn alloy," *Metallurgical and Materials Transactions A*, 29 (4), pp. 1211-1220, 1998.
- [33] J.S. Vetrano, C.A. Lavendar, M. T. Smith, and S. M. Brummer, "Advances in Hot Deformation Texture and Microstructure," J.J. Jonas, T.R. Bieler, and K.J. Bowman, editors, TMS., Warrendale, Pennsylvania, pp. 223-234, 1994.
- [34] H. Imamura and N. Ridley, "Super plasticity in Advanced Materials," ICSAM '91, S. Hori, M. Tokizane, and N. Furushiro, Editors, JSRS, Osaka, pp.453-458, 1994.